


## Entangling Dynamics from Effective Rotor–Spin-Wave Separation in U(1)-Symmetric Quantum Spin Models

Tommaso Roscilde, Tommaso Comparin<sup>✉</sup>, and Fabio Mezzacapo  
*Univ Lyon, Ens de Lyon, CNRS, Laboratoire de Physique, F-69342 Lyon, France*

 (Received 23 March 2023; revised 14 July 2023; accepted 5 September 2023; published 18 October 2023)

The nonequilibrium dynamics of quantum spin models is a most challenging topic, due to the exponentiality of Hilbert space, and it is central to the understanding of the many-body entangled states that can be generated by state-of-the-art quantum simulators. A particularly important class of evolutions is the one governed by U(1)-symmetric Hamiltonians, initialized in a state that breaks the U(1) symmetry—the paradigmatic example being the evolution of the so-called one-axis-twisting (OAT) model, featuring infinite-range interactions between spins. In this Letter, we show that the dynamics of the OAT model can be closely reproduced by systems with power-law-decaying interactions, thanks to an effective separation between the zero-momentum degrees of freedom, associated with the so-called Anderson tower of states, and reconstructing an OAT model, as well as finite-momentum ones, associated with spin-wave excitations. This mechanism explains quantitatively the recent numerical observation of spin squeezing and Schrödinger cat-state generation in the dynamics of dipolar Hamiltonians, and it paves the way for the extension of this observation to a much larger class of models of immediate relevance for quantum simulations.

DOI: [10.1103/PhysRevLett.131.160403](https://doi.org/10.1103/PhysRevLett.131.160403)

*Introduction.*—The controlled generation of many-body entangled states [1–4] is the central feature of quantum many-body devices, such as quantum simulators [5], quantum computers [6], and entanglement-assisted sensors [3], based, e.g., on neutral atoms [7–10], trapped ions [11], or superconducting circuits [12]. Identifying realistic and robust protocols for the scalable preparation of multipartite entangled states [3] is essential for fundamental studies on quantum matter using such devices, as well as for their most advanced applications. In this Letter, we shall specialize to the paradigm of analog quantum simulation based on time-independent Hamiltonians  $\mathcal{H}$ , which generically takes as an input a fiducial, nonentangled initial state  $|\psi(0)\rangle$  and transforms it into an entangled state  $|\psi(t)\rangle = \exp(-i\mathcal{H}t)|\psi(0)\rangle$  via the global unitary evolution. Among the numerous many-body Hamiltonians realizable with state-of-the-art simulators, it is crucial to identify those giving rise to entanglement that can be produced and certified with “polynomial resources”—namely, produced after evolution times  $t$  scaling polynomially with system size and certified via standard observables requiring a polynomial amount of statistics. A further desideratum is for entanglement to be *scalable*, namely, multipartite and with a depth scaling with system size, offering in this way a fundamental test of the scalability of quantum superpositions, as well as the central resource for, e.g., entanglement-assisted metrology [3]. These properties are far from being trivial: generic many-body Hamiltonians evolving random initial factorized states lead to extensive entanglement entropies, which nonetheless can only be certified using

exponentially scaling resources [13,14]. The above requirements can instead be met by exploiting special symmetry properties (exact or approximate) of the many-body Hamiltonian.

A paradigmatic example of an entangling many-body Hamiltonian giving rise to multipartite entangled states with scalable depth is offered by the one-axis-twisting (OAT) model [15]. The latter describes an ensemble of spins of length  $S$  interacting via infinite-range interactions leading to a planar-rotor Hamiltonian,  $\mathcal{H}_{\text{OAT}} = (J^z)^2/(2I)$ . Here  $J^\alpha = \sum_{i=1}^N S_i^\alpha$  ( $\alpha = x, y, z$ ) is the collective-spin operator, and  $I \sim N$  is the macroscopic moment of inertia of the rotor. When the dynamics is initialized in the coherent spin state  $|\text{CSS}_x\rangle = |\psi(0)\rangle = \otimes_{i=1}^N |\rightarrow_x\rangle_i$  polarized along the  $x$  axis, the evolved state  $|\psi(t)\rangle$  develops first spin squeezing, characterized by a squeezing parameter [16]  $\xi_R^2 = N \min_{\perp} \text{Var}(J^{\perp})/\langle J^x \rangle^2$ —where  $\min_{\perp}$  indicates the minimization over the collective-spin components in the  $yz$  plane, perpendicular to the average spin orientation. A parameter  $\xi_R^2 < 1/k$  witnesses  $(k+1)$ -partite entanglement. During the OAT dynamics it reaches a minimal value  $(\xi_R^2)_{\min} \sim N^{-\nu}$  (with  $\nu = 2/3$  for very large system sizes) at a time  $t_{\text{sq}} \sim N^{1/3}$ , therefore realizing scalable multipartite entanglement [15,16]. Moreover, at times  $t_q = 2\pi I/q$  (for  $N$  even, and  $q = 2, \dots, q_{\text{max}}$  with  $q_{\text{max}} \sim \sqrt{N}$ ) the OAT dynamics realizes a cascade of  $q$ -headed Schrödinger’s cat states [17], namely, superpositions of  $q$  coherent spin states rotated around the  $z$  axis by integer multiples of  $2\pi/q$  with respect to the initial  $|\text{CSS}_x\rangle$ .

This sequence culminates with the  $q = 2$  [or Greenberger-Horne-Zeilinger (GHZ)] state  $(|CSS_x\rangle + i|CSS_{-x}\rangle)/\sqrt{2}$  at time  $\pi t$ , featuring  $N$ -partite entanglement.

The OAT model with its infinite-range interactions can be realized literally using atoms or qubits [18–22], and the full sequence of the above-cited entangled states has been realized in recent experiments [22]. Nonetheless, there is mounting evidence that the same dynamics can be obtained using a wide variety of models, such as systems of qubits ( $S = 1/2$  spins), provided that their interactions are sufficiently long ranged, and share with the OAT model its fundamental U(1) symmetry. OAT-like squeezing dynamics has been theoretically reported in XXZ models with power-law-decaying interactions [23–27], and the appearance of the whole cascade of  $q$ -headed cat states has been demonstrated by us for dipolar interactions in 2D [26]. Moreover scalable spin squeezing has been recently demonstrated in experiments on 2D Rydberg atoms with dipolar interactions (Ref. [28]). Yet a quantitative understanding of the persistence of OAT-like dynamics beyond the OAT model is still lacking, in spite of its fundamental importance in order to establish many-body Hamiltonians as potential resources of scalable multipartite entanglement.

In this Letter, we offer a quantitative theoretical insight into this problem, by highlighting an effective mechanism of “separation of variables” taking place in a broad class of models with U(1) symmetry. Making use of a spin-boson mapping, the spin degrees of freedom can be decomposed into a zero-momentum component, reconstructing an effective OAT model when all nonlinearities are properly accounted for; and finite-momentum components, which reconstruct linear spin-wave (SW) excitations at the lowest order in the expansion of the Hamiltonian in powers of bosonic operators. Neglecting the coupling between zero- and finite-momentum bosons (justified when SW excitations are weakly populated) leads to a rotor–spin-wave (RSW) separation scheme: this scheme predicts an additive structure of most salient observables and entanglement entropies, justifying how the full-fledged OAT dynamics can emerge in systems with spatially decaying interactions. The predictions of RSW theory are quantitatively confirmed by time-dependent variational Monte Carlo (tVMC) results in the relevant case of dipolar interactions in two-dimensions—for which tVMC is very accurate, as shown by us in Ref. [26].

*From spins to bosons: rotor–spin-wave separation.*—In this Letter, we focus on the XXZ model for quantum spin lattices,

$$\mathcal{H}_{XXZ} = -\sum_{i<j} J_{ij}(S_i^x S_j^x + S_i^y S_j^y + \Delta S_i^z S_j^z), \quad (1)$$

where  $J_{ij}$  is an arbitrary matrix of ferromagnetic couplings,  $J_{ij} \geq 0$ , and  $\Delta$  is the anisotropy parameter. Throughout the rest of this Letter, the sites  $i, j$  are defined on a periodic

lattice with  $N = L^d$  sites in  $d$  dimensions. In order to quantitatively relate the XXZ model to the OAT one, we first map locally the spins onto Holstein-Primakoff (HP) bosons,  $S_i^x = S - n_i$ ,  $S_i^y = (\sqrt{2S - n_i} b_i + \text{H.c.})/2$ , and  $S_i^z = (\sqrt{2S - n_i} b_i - \text{H.c.})/(2i)$  ( $n_i = b_i^\dagger b_i$ ), where  $b_i, b_i^\dagger$  are bosonic operators, and then we move to momentum space for the bosonic operators,  $b_i = N^{-1/2} \sum_q e^{iq \cdot r_i} b_q$ . The XXZ Hamiltonian expressed in terms of HP bosons has *a priori* a highly nonlinear form; yet the importance of nonlinearities can be very different when looking at zero-momentum bosons versus finite-momentum ones. By construction, the  $|CSS_x\rangle$  state coincides with the vacuum of all HP bosons, and the dynamics initialized in this state has the major effect of depolarizing the collective spin, namely, of letting  $\langle J^x \rangle$  relax to zero, under proliferation of bosons. Ferromagnetic couplings for the  $x$  and  $y$  spin components imply that the lowest-energy bosons have zero momentum, so that one should expect a much faster proliferation of these bosons compared to finite-momentum ones, so that, in practice, for all times (except at the very start)  $\langle b_0^\dagger b_0 \rangle \gg \langle b_{q \neq 0}^\dagger b_{q \neq 0} \rangle$ . Hence nonlinearities for the zero-momentum bosons should be handled with greatest care. As detailed in the Supplemental Material [29] (see also Ref. [31]), *all* the terms in the bosonic Hamiltonian containing exclusively  $b_0$  and  $b_0^\dagger$  bosons can be resummed to reconstruct a planar-rotor (or OAT) model,

$$\mathcal{H}_R = E_{0,R} + \frac{(K^z)^2}{2I}, \quad (2)$$

where  $E_{0,R}$  is the rotor ground-state energy, and  $\mathbf{K}$  is an angular momentum operator of macroscopic length  $NS$ , associated with the zero-momentum bosons, namely,  $K^x = NS - b_0^\dagger b_0$ ,  $K^y = (\sqrt{2NS - n_0} b_0 + \text{H.c.})/2$ , and  $K^z = (\sqrt{2NS - n_0} b_0 - \text{H.c.})/(2i)$ , and the moment of inertia of the rotor variable is given by  $1/(2I) = J_{q=0}(1 - \Delta)/[2(N - 1)]$  [29], where  $J_q = N^{-1} \sum_{ij} e^{iq \cdot (r_i - r_j)} J_{ij}$  [32]. On the other hand, upon linearizing the Hamiltonian in terms of the finite-momentum bosons, one obtains

$$\mathcal{H}_{XXZ} = \mathcal{H}_R + \mathcal{H}_{SW} + \mathcal{O}(n_0 n_{q \neq 0}), \quad (3)$$

where  $\mathcal{H}_{SW} = \sum_{q \neq 0} [A_q b_q^\dagger b_q + \frac{1}{2} B_q (b_q b_{-q} + b_q^\dagger b_{-q}^\dagger)]$  is the quadratic SW Hamiltonian, with  $A_q = S[J_0 - J_q(1 + \Delta)/2]$  and  $B_q = -J_q S(1 - \Delta)/2$  [33].

The central assumption of the RSW scheme is that the most important nonlinearities in the system are all contained in  $\mathcal{H}_R$ , while the further nonlinear terms are negligible. This leads to the additive structure of Eq. (3), implying an effective separation between a nonlinear rotor and linear SWs. Discarding the same kinds of terms for all the quantities of interest leads to a similarly additive structure: e.g., we obtain that  $\langle J^x \rangle = \langle K^x \rangle - N_{FM}$ ,

where  $N_{\text{FM}} = \sum_{q \neq 0} \langle b_q^\dagger b_q \rangle$  is the total number of finite-momentum (FM) bosons;  $\text{Var}(J^x) \approx \text{Var}(K^x) - 2(NS - \langle K^x \rangle)N_{\text{FM}} - N_{\text{FM}}^2$  and  $\text{Var}(J^\perp) \approx \text{Var}(K^\perp)$ . When the ground state of the XXZ Hamiltonian breaks the  $U(1)$  symmetry in the thermodynamic limit (e.g., for  $|\Delta| < 1$  in two dimensions), the low-lying spectrum is expected to feature a so-called Anderson tower of states (ToS) [34,35], possessing the same structure as that of an OAT model,  $E_{\text{ToS}}(J^z) = E_0 + (J^z)^2/I_{\text{ToS}}$ . The fact that  $\langle (J^z)^2 \rangle \approx \langle (K^z)^2 \rangle$  shows that the spectrum of the rotor Hamiltonian (2) reconstructs explicitly the Anderson ToS, albeit with  $I \neq I_{\text{ToS}}$  in general. This discrepancy can be understood from the residual coupling between SW and rotor that we discard and which can be thought of as renormalizing the bare moment of inertia of the rotor. In the following, we shall redefine the rotor variable so as to take into account this renormalization, namely,  $I \rightarrow I_{\text{ToS}}$ . We detail in the Supplemental Material [29] how to systematically reconstruct  $I_{\text{ToS}}$  for all the system sizes  $N$  we considered.

*Dynamics of the dipolar XX model.*—Within the RSW scheme, the quench dynamics of the system is then solved at a polynomial cost by evolving separately the rotor variable [with a  $(2NS + 1)$ -dimensional Hilbert space] and the SW ones (whose dynamics can be solved for

analytically [36]). We then apply the RSW approach to the relevant case of the dipolar  $S = 1/2$  XX model, corresponding to  $\Delta = 0$  and  $J_{ij} = J|\mathbf{r}_i - \mathbf{r}_j|^{-3}$ , in the case of a square lattice. This model is literally realized in Rydberg-atom arrays with resonant interactions [8,28,37], but many more platforms are described by XXZ dipolar models [38,39]. Figure 1 shows a systematic comparison of our RSW results with those of tVMC based on a pair-product ansatz [25,26,40]. Figure 1(a) shows the depolarizing dynamics of the average collective spin  $\langle J^x \rangle$ , which admits an exact additive structure in terms of the zero- and finite-momentum components. We observe that the population of zero-momentum bosons becomes very quickly much larger than that of all the finite-momentum ones taken together, validating the basic assumption of RSW theory. Subtracting the boson populations from the initial average spin  $N/2$  gives a prediction for  $\langle J^x \rangle$  in very good agreement with tVMC, especially at short times—while at longer times the neglect of the coupling between rotor and SW leads to deviations from tVMC. The short-time squeezing dynamics is then examined in Fig. 1(b), showing that RSW and tVMC are in nearly perfect agreement. In fact, due to the very weak population of finite-momentum bosons, the squeezing parameter is almost fully accounted for by the

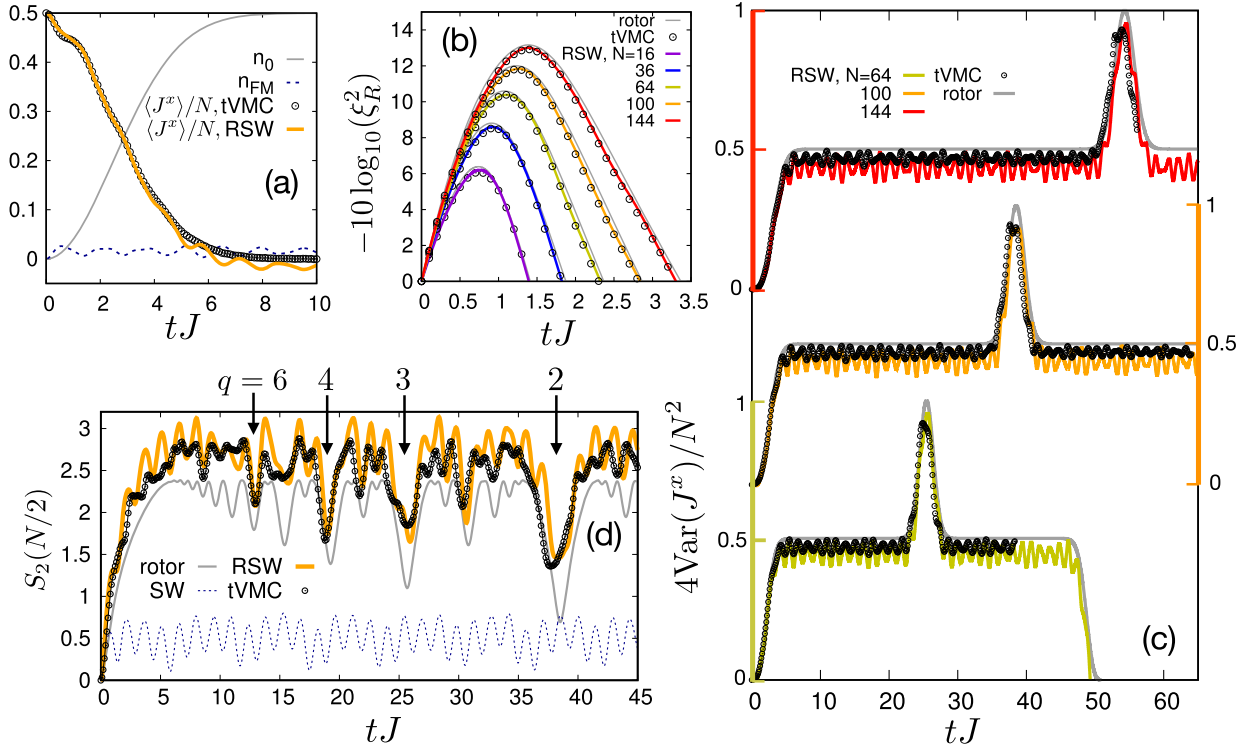


FIG. 1. Dynamics of the 2D dipolar XX model. (a) Dynamics of the average magnetization  $\langle J^x \rangle$  for  $N = 100$  spins, comparing RSW and tVMC results. The graph also shows the density of zero-momentum bosons  $n_0 = \langle b_0^\dagger b_0 \rangle/N$  and finite-momentum ones  $n_{\text{FM}} = N_{\text{FM}}/N$ . (b) Spin squeezing parameter for various system sizes; in this and further panels, the rotor results correspond to those of an OAT model with moment of inertia  $I_{\text{ToS}}$ . (c) Dynamics of the magnetization variance. (d) Dynamics of the half-system Rényi entropy for a system of  $N = 100$  spins, showing the separate rotor and SW contributions whose sum leads to the RSW prediction. The arrows mark the time of appearance of some of the  $q$ -headed cat states.

rotor variable alone. The SW contribution enters uniquely via  $N_{\text{FM}}$  in  $\langle J^x \rangle^2$ ; yet it provides the slight renormalization that fixes the discrepancy between the bare rotor results and the tVMC ones.

Figure 1(c) goes beyond the short time squeezing dynamics and looks instead at the evolution of  $\text{Var}(J^x)$ , which attains first a plateau at  $N^2/8$  in the OAT dynamics, followed by a sharp peak of height  $N^2/4$  at time  $\pi I$ , which corresponds to the appearance of a GHZ state. The RSW results show that the SW contribution to the variance introduces a reduction in the plateau value, as well as oscillations at the characteristic frequency of evolution of  $N_{\text{FM}}$ . This behavior reflects closely that of the tVMC results, with a very clear correspondence in the fluctuating part, although the amplitude of the oscillations appears to be overestimated by the RSW results. Finally, both the tVMC results and the RSW ones show the peak associated with the appearance of the GHZ-like state, with a height slightly reduced by the SW contribution, which quantitatively accounts for the deviation from the bare rotor results. The RSW scenario hence justifies the persistence of the formation of a GHZ-like state up to  $N = 144$  spins, as already reported by us in Ref. [26]. The formation of the GHZ-like state, along with that of  $q$ -headed cat states with  $q > 2$  at earlier times, can also be tracked by inspecting the half-system Rényi entanglement entropy,  $S_2(N/2) = -\log \text{Tr}(\rho_{N/2}^2)$ , where  $\rho_{N/2}$  is the reduced state of a rectangle of  $L \times L/2 = N/2$  spins. Within the RSW approach, this entropy is strictly additive, and it is composed of a rotor contribution and a SW one [33,36,41]. Figure 1(d) shows that the addition of the rotor and SW entropies accounts very closely for the tVMC results. In particular, the rotor entropy exhibits a succession of dips occurring at times  $t_q = 2\pi I/q$  corresponding to the formation of the  $q$ -headed cat states [41], which is nicely reflected by the tVMC results as well, with superposed fluctuations coming from the SW contribution. It is worth noticing that the rotor entropy is  $\mathcal{O}(\log N)$  (due to the polynomial Hilbert space dimensions for the rotor), while the maximum SW entropy is  $\mathcal{O}(N)$  (volume-law scaling); nonetheless, the SW excitations are so dilute that the entropy is clearly dominated by the rotor contribution for the sizes ( $N \sim 100$ ) considered here.

A final element of comparison concerns the dynamics of correlations. Figure 2 focuses, in particular, on the correlation functions  $C^{zz}(\mathbf{d}) = \langle S_i^z S_{i+d}^z \rangle$  and  $C^{yy}(\mathbf{d}) = \langle S_i^y S_{i+d}^y \rangle$  for spin components perpendicular to the collective-spin orientation—see also the Supplemental Material [29] for further extended data. The RSW approach reveals that these correlations possess a very distinct origin: for the system size considered here ( $N = 100$ ), the  $C^{yy}$  correlations are dominated by the rotor contribution  $\langle (K^y)^2 \rangle / N^2$ , which is independent of the distance, while their subdominant spatial modulation comes from the SW contribution. On the other hand, the  $C^{zz}$  correlations are exclusively given by

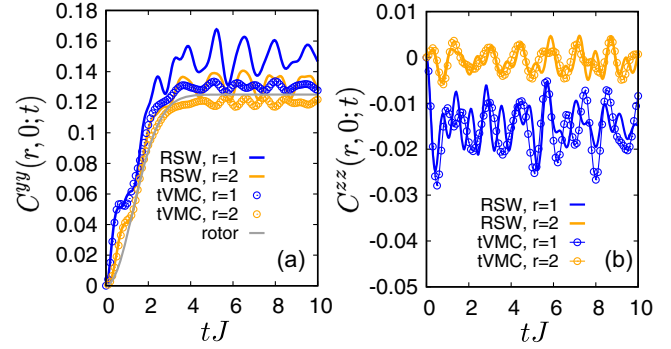


FIG. 2. Correlation dynamics for the 2D dipolar  $XX$  model. (a)  $C^{yy}$  correlations at distance  $r = 1$  and 2. (b)  $C^{zz}$  correlations for the same distances as in (a).

the SW contribution, because the rotor Hamiltonian commutes with the  $S_i^z$  operators; therefore, correlations among them cannot develop under the rotor dynamics. This observation justifies why SW theory alone, neglecting any zero mode, can successfully describe the  $C^{zz}$  correlations [36]. Figure 2 shows that SW excitations add a spatial modulation and an oscillating behavior on top of the rotor contribution for the  $C^{yy}$  correlations, while they fully account for the  $C^{zz}$  correlations; this justifies also why the latter correlations are roughly an order of magnitude smaller than the  $C^{yy}$  ones. Our results suggest also that a Fourier analysis of the  $C^{zz}$  correlations via quench spectroscopy [42,43] allows one to reconstruct selectively the dispersion relation of the finite-momentum SW excitations; while the same analysis for the  $C^{yy}$  correlations would reveal as well the ToS excitations at zero momentum. The fact that  $C^{yy}$  correlations are dominated by the rotor dynamics is apparently in contradiction with the picture of correlation dynamics as being governed by propagating quasiparticles [44,45]; nonetheless, the rotor dynamics is parametrically slower the larger the size  $N$ , so that correlation spreading keeps a causal structure, as further discussed in the Supplemental Material [29].

*Dynamical transition in  $XX$  chains with power-law interactions.*—The above results have shown that the dynamics of the dipolar  $XX$  model in  $d = 2$  is dominated by the rotor contribution; this aspect justifies *a posteriori* the assumptions of RSW theory and explains its success for this specific example. Remarkably, RSW theory can also signal the appearance of a dynamical transition from an OAT-like dynamics to a non-OAT one, when its assumptions fail at long times. We demonstrate this aspect in the case of the  $XX$  model with power-law interactions,  $J_{ij} = J|r_i - r_j|^{-\alpha}$ , cast on a  $d = 1$  lattice. As already shown in Refs. [25,27], this model exhibits OAT-like dynamics with scalable squeezing (i.e., featuring a minimum of the  $\xi_R^2$  parameter, which scales with system size) for  $\alpha \lesssim 1.6$ ; and absence of scalable squeezing for larger values of  $\alpha$ . Figure 3 shows the minimum value of the  $\xi_R^2$

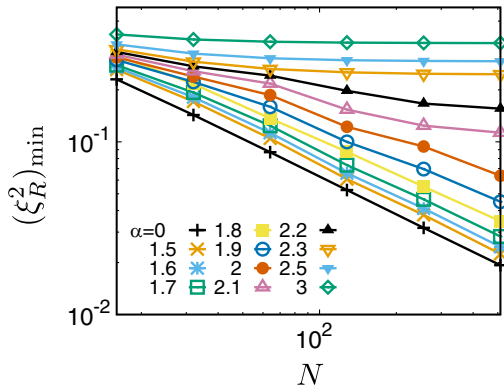


FIG. 3. Dynamical transition in the 1D  $XX$  model with power-law interactions. Scaling of the minimum squeezing parameter for various values of the power  $\alpha$  for the decay of interactions.

parameter achieved during the RSW dynamics [46]. Two distinct scaling behaviors are clearly exhibited: one compatible with OAT dynamics at small  $\alpha$ ; and one compatible with non-scalable squeezing at large  $\alpha$ —with a seemingly smooth crossover between the two regimes occurring around  $\alpha \approx 2$ . Hence RSW theory overestimates the value of  $\alpha$  at which scalable squeezing is lost. The non-scaling regime is due to the proliferation of SWs, leading to a fast depolarization of the average collective spin  $\langle J^x \rangle$ , which manifests the absence of long-range order for the  $\alpha - XX$  chains model at the energy corresponding to the initial state [27]. This depolarization happens on a timescale independent of system size, i.e., parametrically faster than the onset of scaling for the minimum variance of the transverse spin components [occurring at a time  $\sim \mathcal{O}(N^{1/3})$  within RSW theory]. The breakdown of OAT scaling in the squeezing signals that the RSW predictions cease to be quantitative at longer times.

*Conclusions.*—In this Letter, we have demonstrated that the entangling dynamics of the infinite-range one-axis-twisting model can be reproduced with minor alterations by  $U(1)$ -symmetric spin models with power-law-decaying interactions, thanks to an effective separation between zero-momentum degrees of freedom, possessing the spectrum of a planar-rotor variable, and finite-momentum ones, corresponding to spin-wave excitations. This effective separation of variable is always justified at short times, and it remains justified even for macroscopic [ $\mathcal{O}(N)$ ] times when the spin-wave excitations are weakly populated, allowing for the appearance of scalable spin squeezing, as well as scalable catlike states. The same separation scheme, or extensions thereof, can be applied to other models (such  $Z_2$ - or  $SU(2)$ -symmetric ones), and it can improve systematically on linear spin-wave dynamics whenever the latter is applicable. The quantitative success of our approach in describing the dynamics of, e.g., dipolar spins in two dimensions suggests that this and similar systems, albeit not being properly integrable, undergo a

rather peculiar dynamics at low energy. This dynamics is dominated by persistent spin-wave oscillations and approximate recurrences at times  $\mathcal{O}(N)$ —as opposed to Poincaré times  $\mathcal{O}[\exp(N)]$ —which reflect the reduced Hilbert space of the rotor variable. While rotor and spin waves should eventually come to thermalize with each other thanks to their residual coupling, the timescales over which such thermalization occurs are currently unknown to us. Our findings suggest that effective rotor–spin-wave decoupling represents the mechanism by which a very large class of power-law interacting Hamiltonians implemented by quantum simulators—including Rydberg atoms [8], magnetic atoms [39], trapped ions [11,47], superconducting circuits [22]—can evade standard thermalization at low energy. And, by virtue of this mechanism, they can act as entangling resources producing scalable multipartite entanglement of interest for fundamental studies, as well as for potential metrological applications.

Fruitful discussions with M. Block, G. Borner, A. Browaeys, C. Chen, G. Emperauger, T. Lahaye, N. Yao, and B. Ye are gratefully acknowledged. This work is supported by ANR (EELS project), QuantERA (MAQS project), and PEPR-Q (QubitAF project). All numerical simulations have been performed on the PSMN cluster at the ENS of Lyon.

- [1] R. Horodecki, P. Horodecki, M. Horodecki, and K. Horodecki, *Rev. Mod. Phys.* **81**, 865 (2009).
- [2] O. Gühne and G. Tóth, *Phys. Rep.* **474**, 1 (2009).
- [3] L. Pezzè, A. Smerzi, M. K. Oberthaler, R. Schmied, and P. Treutlein, *Rev. Mod. Phys.* **90**, 035005 (2018).
- [4] N. Friis, G. Vitagliano, M. Malik, and M. Huber, *Nat. Rev. Phys.* **1**, 72 (2019).
- [5] I. M. Georgescu, S. Ashhab, and F. Nori, *Rev. Mod. Phys.* **86**, 153 (2014).
- [6] M. A. Nielsen and I. L. Chuang, *Quantum Computation and Quantum Information* (Cambridge University Press, Cambridge, England, 2010).
- [7] C. Gross and I. Bloch, *Science* **357**, 995 (2017).
- [8] A. Browaeys and T. Lahaye, *Nat. Phys.* **16**, 132 (2020).
- [9] F. Schäfer, T. Fukuhara, S. Sugawa, Y. Takasu, and Y. Takahashi, *Nat. Rev. Phys.* **2**, 411 (2020).
- [10] A. Kaufman and K.-K. Ni, *Nat. Phys.* **17**, 1324 (2021).
- [11] C. Monroe, W. C. Campbell, L.-M. Duan, Z.-X. Gong, A. V. Gorshkov, P. W. Hess, R. Islam, K. Kim, N. M. Linke, G. Pagano *et al.*, *Rev. Mod. Phys.* **93**, 025001 (2021).
- [12] J. García-Ripoll, *Quantum Information and Quantum Optics with Superconducting Circuits* (Cambridge University Press, Cambridge, England, 2022).
- [13] A. M. Kaufman, M. E. Tai, A. Lukin, M. Rispoli, R. Schittko, P. M. Preiss, and M. Greiner, *Science* **353**, 794 (2016).
- [14] T. Brydges, A. Elben, P. Jurcevic, B. Vermersch, C. Maier, B. P. Lanyon, P. Zoller, R. Blatt, and C. F. Roos, *Science* **364**, 260 (2019).
- [15] M. Kitagawa and M. Ueda, *Phys. Rev. A* **47**, 5138 (1993).

- [16] D. J. Wineland, J. J. Bollinger, W. M. Itano, and D. J. Heinzen, *Phys. Rev. A* **50**, 67 (1994).
- [17] G. S. Agarwal, R. R. Puri, and R. P. Singh, *Phys. Rev. A* **56**, 2249 (1997).
- [18] M. F. Riedel, P. Böhi, Y. Li, T. W. Hänsch, A. Sinatra, and P. Treutlein, *Nature (London)* **464**, 1170 (2010).
- [19] C. Gross, *J. Phys. B* **45**, 103001 (2012).
- [20] M. A. Norcia, R. J. Lewis-Swan, J. R. K. Cline, B. Zhu, A. M. Rey, and J. K. Thompson, *Science* **361**, 259 (2018).
- [21] B. Braverman, A. Kawasaki, E. Pedrozo-Peñafiel, S. Colombo, C. Shu, Z. Li, E. Mendez, M. Yamoah, L. Salvi, D. Akamatsu *et al.*, *Phys. Rev. Lett.* **122**, 223203 (2019).
- [22] C. Song, K. Xu, H. Li, Y.-R. Zhang, X. Zhang, W. Liu, Q. Guo, Z. Wang, W. Ren, J. Hao *et al.*, *Science* **365**, 574 (2019).
- [23] M. Foss-Feig, Z.-X. Gong, A. V. Gorshkov, and C. W. Clark, [arXiv:1612.07805](https://arxiv.org/abs/1612.07805).
- [24] M. A. Perlin, C. Qu, and A. M. Rey, *Phys. Rev. Lett.* **125**, 223401 (2020).
- [25] T. Comparin, F. Mezzacapo, and T. Roscilde, *Phys. Rev. A* **105**, 022625 (2022).
- [26] T. Comparin, F. Mezzacapo, and T. Roscilde, *Phys. Rev. Lett.* **129**, 150503 (2022).
- [27] M. Block, B. Ye, B. Roberts, S. Chern, W. Wu, Z. Wang, L. Pollet, E. J. Davis, B. I. Halperin, and N. Y. Yao, [arXiv:2301.09636](https://arxiv.org/abs/2301.09636).
- [28] G. Bornet, G. Emperauger, C. Chen, B. Ye, M. Block, M. Bintz, J. A. Boyd, D. Barredo, T. Comparin, F. Mezzacapo *et al.*, [arXiv:2303.08053](https://arxiv.org/abs/2303.08053).
- [29] See Supplemental Material at <http://link.aps.org/supplemental/10.1103/PhysRevLett.131.160403> for details about (1) the reconstruction of the OAT model for zero-momentum bosons and (2) the time evolution of spin-spin correlations, which includes Ref. [30].
- [30] L. Cevolani, J. Despres, G. Carleo, L. Tagliacozzo, and L. Sanchez-Palencia, *Phys. Rev. B* **98**, 024302 (2018).
- [31] T. Roscilde, T. Comparin, and F. Mezzacapo, companion article, *Phys. Rev. B* **108**, 155130 (2023).
- [32] The moment of inertia of the rotor can become negative when  $\Delta > 1$ , signaling the fact that the low-energy physics of the system is no longer akin to that of a rotor in the  $xy$  plane, because the system develops Ising-like ferromagnetism along  $z$  instead. Yet a negative moment of inertia is not an issue when considering the real-time dynamics.
- [33] I. Frérot, P. Naldesi, and T. Roscilde, *Phys. Rev. B* **95**, 245111 (2017).
- [34] P. W. Anderson, *Basic Notions of Condensed Matter Physics* (Taylor & Francis, Boca Raton, FL, 1997).
- [35] H. Tasaki, *J. Stat. Phys.* **174**, 735 (2018).
- [36] I. Frérot, P. Naldesi, and T. Roscilde, *Phys. Rev. Lett.* **120**, 050401 (2018).
- [37] C. Chen, G. Bornet, M. Bintz, G. Emperauger, L. Leclerc, V. S. Liu, P. Scholl, D. Barredo, J. Hauschild, S. Chatterjee *et al.*, *Nature (London)* **616**, 691 (2023).
- [38] K. R. A. Hazzard, S. R. Manmana, M. Foss-Feig, and A. M. Rey, *Phys. Rev. Lett.* **110**, 075301 (2013).
- [39] L. Chomaz, I. Ferrier-Barbut, F. Ferlaino, B. Laburthe-Tolra, B. L. Lev, and T. Pfau, *Rep. Prog. Phys.* **86**, 026401 (2023).
- [40] J. Thibaut, T. Roscilde, and F. Mezzacapo, *Phys. Rev. B* **100**, 155148 (2019).
- [41] H. Kurkjian, K. Pawłowski, A. Sinatra, and P. Treutlein, *Phys. Rev. A* **88**, 043605 (2013).
- [42] R. Menu and T. Roscilde, *Phys. Rev. B* **98**, 205145 (2018).
- [43] L. Villa, J. Despres, and L. Sanchez-Palencia, *Phys. Rev. A* **100**, 063632 (2019).
- [44] P. Calabrese and J. Cardy, *Phys. Rev. Lett.* **96**, 136801 (2006).
- [45] M. Cheneau, P. Barmettler, D. Poletti, M. Endres, P. Schauß, T. Fukuhara, C. Gross, I. Bloch, C. Kollath, and S. Kuhr, *Nature (London)* **481**, 484 (2012).
- [46] For these calculations, for the sake of simplicity, we considered a rotor with bare moment of inertia.
- [47] J. Franke, S. R. Muleady, R. Kaubruegger, F. Kranzl, R. Blatt, A. M. Rey, M. K. Joshi, and C. F. Roos, [arXiv:2303.10688](https://arxiv.org/abs/2303.10688).